ELSEVIER

Polymer 40 (1999) 5043–5049

polymer

Microstructure and mechanical properties of hot-air drawn poly(ethylene-2,6-naphthalate) fibers

Akihiro Suzuki*, Yukio Nakamura, Toshio Kunugi

Department of Applied Chemistry and Biotechnology, Faculty of Engineering, Yamanashi University, 4-3-11 Takeda, Kofu 400-8511, Japan

Received 3 June 1998; received in revised form 10 August 1998; accepted 14 October 1998

Abstract

A hot-air (HA) drawing method has been applied to poly(ethylene-2,6-naphthalate) (PEN) fibers in order to improve their mechanical properties. The HA drawing was carried out by blowing hot-air controlled at a constant temperature against an original PEN fiber connected to a weight. As the hot-air blew against the fiber at a flow rate of 90 l/min, the fiber elongated instantaneously at a strain rate in the range from 15.9 to 25.2 s^{-1}. The strain rate during the HA drawing increased with increasing drawing temperature and applied tension. When the HA drawing was carried out at a drawing temperature of 250°C under an applied tension of 17.4 MPa, the strain rate had the highest value of 25.2 s^{-1}. Draw ratio, birefringence, crystallite orientation factor, and mechanical properties increased as the strain rate increased. The fiber drawn at the highest strain rate had a birefringence of 0.436, degree of crystallinity of 45%, tensile modulus of 29 GPa, and dynamic storage modulus of 30 GPa at 25°C. The mechanical properties of the fiber obtained had almost the same values as those of zone-annealed PEN fibers.

Keywords: Poly(ethylene-2,6-naphthalate) fiber; Hot-air drawing; Drawing conditions

1. Introduction

Poly(ethylene-2,6-naphthalate) (PEN) is one of high temperature semicrystalline thermoplastic polymers that combine the properties of superior chemical resistance, flame resistance, and mechanical strength. Its mechanical properties, glass transition temperature, and melting point are higher than those of poly(ethylene terephthalate) (PET), because PEN has a naphthalene ring instead of the benzene ring in PET.

There are two known crystal modifications [1]; an α-form and a β-form. The α-form [2] is a triclinic unit cell with the unit-cell parameters a = 0.651 nm, b = 0.575 nm, c = 1.32 nm, $\alpha = 81.33°$, $\beta = 144°$, and $\gamma = 100°$. One chain passes through each unit cell. The β-form [1] is also a triclinic unit cell with unit-cell parameters a = 0.926 nm, b = 1.559 nm, c = 1.273 nm, $\alpha = 121.6°$, $\beta = 95.57°$, and $\gamma = 122.52°$. Four chains pass through each cell. The chains are not completely extended; every naphthalene ring is twisted by 180°.

Numerous studies [3–11] have been undertaken to investigate the crystalline structure, morphology, thermal stability, and crystallization kinetics of PEN. Buchner et al. [11] studied the kinetics of crystallization and melting behavior of PEN. They found that at crystallization temperatures up to 200°C only the α-form was formed. At the crystallization temperature, the β-form was obtained if the material had been molten at 280°C, while the α-form was formed if the temperature of the melt was raised to 320°C. The α-form and β-form had almost the same melting point, and no change of crystal morphology was observed during annealing. The half times of crystallization as functions of temperature showed a broad minimum ranging from 180 to 240°C. Few investigations [12–16] have been carried out on the mechanical properties of PEN fibers. Ghanem and Porter [12] studied the cold crystallization and thermal shrinkage of PEN uniaxially drawn by solid-state coextrusion. They found that the onset of crystallization depended markedly on the drawing conditions, and that thermal shrinkage also showed a strong dependence on drawing conditions. Nagai et al. [14,15] studied the superstructure and mechanical properties of the PEN fibers prepared by high-speed spinning in the 1,000–5,000 m/min range. We applied a zone-drawing/zone-annealing to the PEN fibers and reported their superstructure and mechanical properties [16].

We so far proposed some of the techniques leading to

* Corresponding author. Tel.: + 81-552-8556; fax: + 81-552-8556.
E-mail address: a-suzuki@ab11.yamanashi.ac.jp (A. Suzuki)

0032-3861/99/$ - see front matter
PII: S0032-3861(98)00728-9

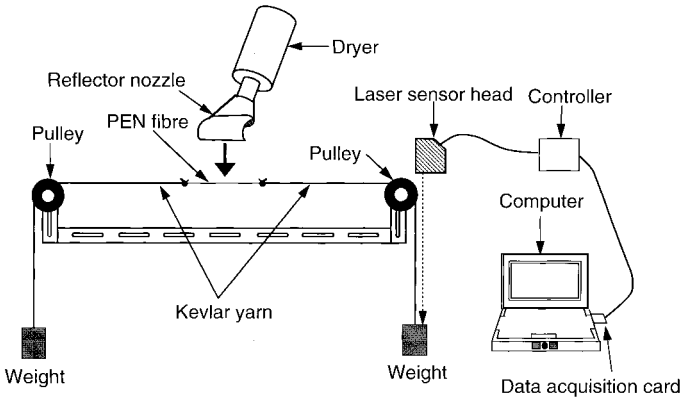

Fig. 1. Schematic diagram of the instrument used for the hot-air drawing.

high-modulus and high-strength fibers: a zone-drawing/zone-annealing [17], a high-tension annealing [18], a continuous zone-drawing/zone-annealing [19], and a vibrating hot-drawing method [20]. These methods were applied to various polymers and were proved to be effective in improving their mechanical properties. We propose newly a hot-air (HA) drawing method to produce high-modulus and high-strength polymers. The HA drawing is characterized by extremely rapid drawing and has the same effect on the improvement of mechanical properties as the zone-drawing/zone-annealing treatment.

It is the purpose of the present paper to discuss the effect of strain rate on the mechanical properties and superstructure of hot-air drawn (HAD) PEN fiber and to produce a high-performance PEN fiber.

2. Experimental

2.1. Material

The original material used in the present study was the as-spun PEN fibers supplied by Teijin Ltd. The original fiber had a diameter of about 0.379 mm, degree of crystallinity of 4%, birefringence of 3×10^{-3}, and an intrinsic viscosity of 0.63 dl/g. The original fiber was found to be amorphous and isotropic from a wide-angle X-ray diffraction photograph.

2.2. HA drawing method

A schematic of the instrument used for these experiments is given in Fig. 1. The instrument consists of a dryer with an 8 cm width reflector nozzle, a laser displacement sensor system, and two fixed pulleys which were horizontally placed 650 mm apart from each other. The dryer is capable of adjusting the temperature within an accuracy of about ± 2°C and the flow rate of the hot-air (maximum flow rate of 230 l/min). Two ends of the original fiber of about 10 cm length were attached to the Kevlar yarns 30 cm long. The Kevlar yarns were able to pass over the fixed pulley and connected to a weight at their other ends. When the weight was added to the fiber, no cold drawing occurred at room temperature. As the dryer was moved downward in order to heat the fiber and then the hot-air was blown against the fiber at a flow rate of about 90 l/min, the fiber elongated instantaneously. Draw ratio was determined by measuring the displacement of the ink marks placed 10 mm apart on the fiber prior to drawing. Drawing time was measured by a laser displacement sensor system. This system consists of a laser sensor head, a controller, a data acquisition card, and a microcomputer. The strain rate was estimated from the drawing time and draw ratio.

2.3. Measurement

Birefringence was measured with a polarizing microscope equipped with a Berek compensator. The X–Z quartz compensator cut from single crystal was additionally used because the highly oriented PEN fiber had higher retardation. The density (ρ) of the fiber was measured at 23°C by a flotation technique using a carbon tetrachloride and toluene mixture. The degree of crystallinity, expressed as a weight fraction (X_w), was obtained using the relation:

$$X_w = \{\rho_c(\rho - \rho_a)\}/\{\rho(\rho_c - \rho_a)\} \times 100 \quad (1)$$

where ρ_c and ρ_a are densities of the crystalline and amorphous phases, respectively. In this measurement, values of 1.407 and 1.325 g/cm^3 were assumed for ρ_c [21] and ρ_a [22], respectively.

Wide-angle X-ray diffraction patterns for the fibers were obtained with a Rigaku X-ray generator and diffractometer equipped with a fiber specimen attachment. The X-ray unit was operated at 40 kV and 20 mA, and the radiation used was Ni-filtered CuK_α. Orientation factors of crystallites (f_c) were evaluated by using the Wilchinsky method [23] from the wide angle X-ray diffraction patterns.

D.s.c. curves were recorded on a Rigaku DSC connected to a TAS 200 system at a heating rate of 10°C/min. All measurements were carried out under a nitrogen purge. The d.s.c. instrument was calibrated with indium.

The thermal shrinkage was measured with a Rigaku

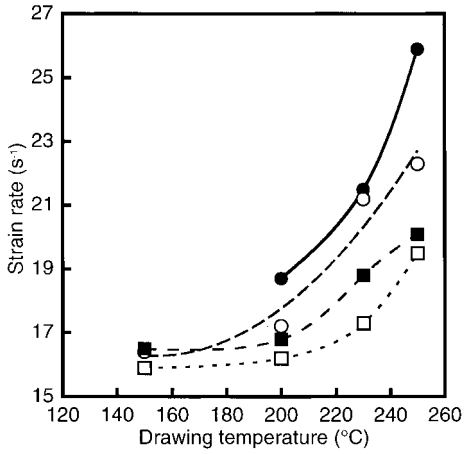

Fig. 2. Changes in strain rate at four different applied tensions (σ_a) with drawing temperature: (□) σ_a = 8.7 MPa; (■) σ_a = 13.0 MPa; (○) σ_a = 15.6 MPa; (●) σ_a = 17.4 MPa.

SS-TMA at a heating rate of 5°C/min. The specimens were 15 mm long and were subject to a stress, 5 g/cm^2 which is the minimum value required to stretch the specimen tightly.

The tensile properties were determined with a Tensilon tensile testing machine. A tensile modulus, tensile strength, and elongation at break were calculated from the stress–strain curves obtained at 23°C and 65% RH. The dynamic viscoelastic properties were measured at 110 Hz with a dynamic viscoelastometer VIBRON DDV-II (Orientec Co. Ltd). Measurements were carried out over a temperature range of 30°C to about 210°C at an interval of 5°C, and the average heating rate was 2°C/min. A single fiber was held in a gauge with a separation of 20 mm length between two jaws.

3. Results and discussion

3.1. Effects of drawing temperature and applied tension on superstructure of HAD fiber

To study the effects of the drawing temperature (T_d) and applied tension (σ_a) on strain rate ($\dot{\varepsilon}$) and superstructure, the HA drawing was carried out at various T_ds and σ_as. Fig. 2 shows the changes in $\dot{\varepsilon}$ at four different σ_as with T_d. The σ_a values at T_d = 150°C have no significant effects on $\dot{\varepsilon}$ and give constant $\dot{\varepsilon}$ values of 16 s^{-1}. Above 200°C $\dot{\varepsilon}$ increases rapidly with increasing σ_a, and the drawing at T_d = 250°C and σ_a = 17.4 MPa gives the highest value of 25.2 s^{-1}.

Fig. 3(a) and (b) show the $\dot{\varepsilon}$ dependence of the draw ratio (λ) and birefringence (Δn) of the hot-air drawn (HAD) fibers obtained under various conditions. λ and Δn of the fiber increase with increasing $\dot{\varepsilon}$, and the HAD fiber drawn at T_d = 250°C under σ_a = 17.4 MPa has the maximum λ (= 7.8) and Δn (= 0.436). These values are approximately equal to those (λ = 8.4, Δn = 0.473) of the zone-annealed PEN fiber reported previously [16]. This indicates that no

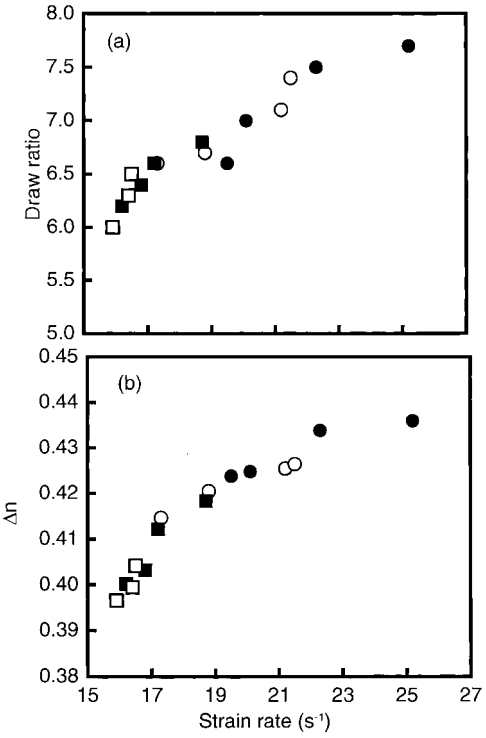

Fig. 3. Changes in (a) draw ratio and (b) birefringence (Δn) of fibers drawn under four different drawing temperatures (T_d) with strain rate: (□) T_d = 150°C; (■) T_d = 200°C; (○) T_d = 230°C; (●) T_d = 250°C.

flow drawing due to sliding of chains occurs in the HA drawing. The values are found to increase unequivocally with $\dot{\varepsilon}$ independent of T_d and σ_a. Despite rapid drawing and only one treatment, the attained Δn value is higher than that (Δn = about 0.25) of the PEN fiber obtained by high-speed spinning [14]. The Δn of the HAD fiber, however, is fairly lower than the intrinsic birefringence (0.604) of the crystalline region calculated theoretically [24].

Fig. 4 shows the relation between Δn and λ of the HAD fibers obtained under various conditions. Δn increases linearly up to high Δn with increasing λ. O'Neill et al. [25] reported that Δn increased gradually with increasing λ at low λ, and it leveled off to reach a saturated value at high λ. In the HA drawing, however, Δn increases linearly up to high λ without such a leveling-off. The linear relation implies that the HA drawing was effective in drawing chain molecules without the relaxation of the orientation resulted from a chain slippage. Ajji et al. [26] studied the orientation and structure of the PET films drawn uniaxially at different strain rates (= 0.0017 ~ 0.083 s^{-1}) at 80°C. They showed that in the fibers drawn at a high drawing rate, no birefringence was observed up to a draw ratio of 3. This fact indicated that the intermolecular linkages are broken down, and consequently molecular chains might slip past one another and flow individually, exhibiting a large deformation without inducing any molecular orientation and crystallization.

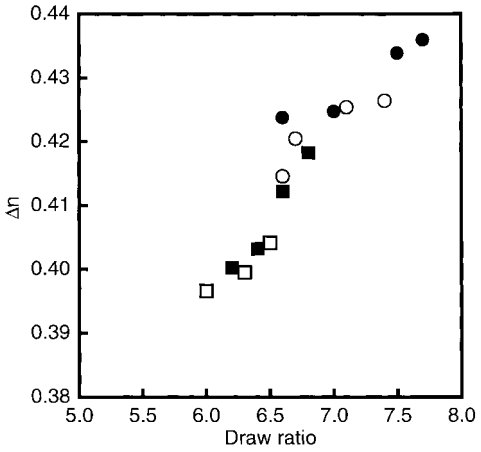

Fig. 4. Relation between birefringence (Δn) and draw ratio for the HAD fibers obtained under various conditions: (□) $T_d = 150$°C; (■) $T_d = 200$°C; (○) $T_d = 230$°C; (●) $T_d = 250$°C.

Fig. 5 shows the changes in the degree of crystallinity (X_w) with $\dot{\varepsilon}$. The X_w value increases with increasing $\dot{\varepsilon}$ at each T_d, but there is no linear relation between X_w and $\dot{\varepsilon}$ at any T_d. The result differs from the linear relation between λ and $\dot{\varepsilon}$, Δn and $\dot{\varepsilon}$, or the crystallite orientation factor and $\dot{\varepsilon}$ described below. The maximum X_w value of the HAD fiber drawn at 250°C was $X_w = 45\%$, which is higher than X_w(= 40%) of the zone-annealed fiber [16]. Ghanem et al. [12] showed that the upper limit of X_w of the PEN fiber drawn uniaxially by solid-state coextrusion was about 48%. Despite drawing of amorphous fiber carried out at T_d = 250°C close to melting point, it is worth noting that the strain-induced crystallization occurs without fluid-like deformation caused slippage among the amorphous chains.

The crystallite orientation factor (f_c) is plotted as a function of $\dot{\varepsilon}$ in Fig. 6. The f_c value reaches up to a high value by the HA drawing and unequivocally depends on $\dot{\varepsilon}$. The HAD fiber drawn at $\dot{\varepsilon} = 25.1\ s^{-1}$ has a maximum f_c value of 0.951. Since the HA drawing is carried out at T_d close to the melting point (= 268°C) of the original fiber, f_c reaches

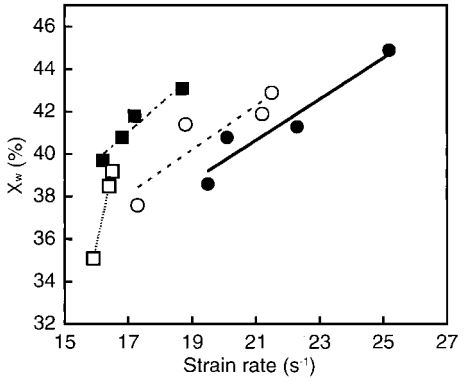

Fig. 5. Changes in a degree of crystallinity (X_w) with strain rate for the HAD fibers obtained under various conditions: (□) $T_d = 150$°C; (■) $T_d = 200$°C; (○) $T_d = 230$°C; (●) $T_d = 250$°C.

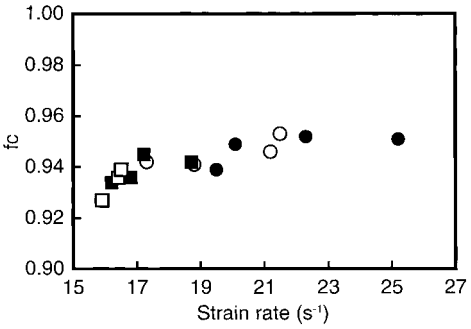

Fig. 6. Changes in crystallite orientation factor (f_c) with strain rate for the HAD fibers obtained under various conditions: (□) $T_d = 150$°C; (■) $T_d = 200$°C; (○) $T_d = 230$°C; (●) $T_d = 250$°C.

such a high value. The result also shows that the alignment of molecular chains in the draw direction predominate over molecular relaxation due to chain slippage.

Fig. 7(a) shows the wide-angle X-ray diffraction equatorial patterns for the HAD fibers obtained under four different σ_as at $T_d = 250$°C and Fig. 7(b) those under $\sigma_a = 17.4$ MPa at three different T_d. The diffraction patterns become slightly sharp with increasing σ_a or T_d. Three reflections (010, 100, and 110) attributed to the α-form [27] are observed in the equator, but no (020) reflection due to the β-form [11] is

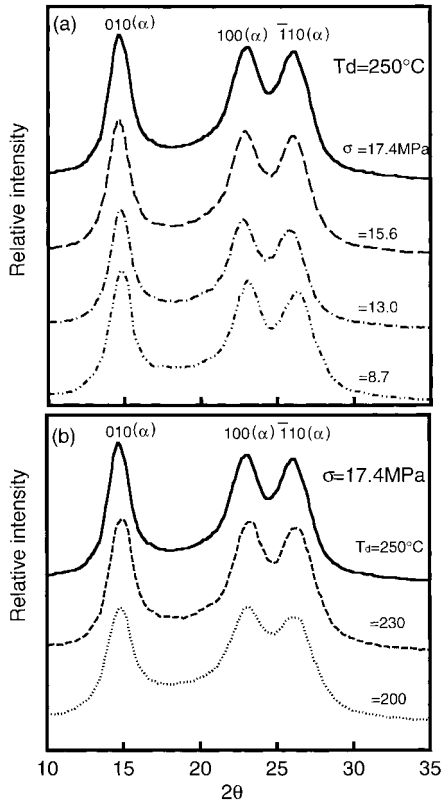

Fig. 7. Wide-angle X-ray diffraction equatorial patterns of the HAD fibers under different conditions: (a) the HAD fibers under four different applied tensions (σ_a) at a drawing temperature (T_d) of 250°C; (b) the HAD fibers at four different T_d under $\sigma_a = 17.4$ MPa.

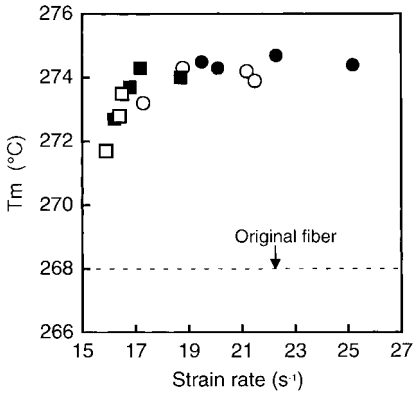

Fig. 8. Change in a melting point (T_m) with strain rate for the fibers obtained under various conditions: (□) T_d = 150°C; (■) T_d = 200°C; (○) T_d = 230°C; (●) T_d = 250°C.

observed in the equator ($2\theta = 18.7°$). It will be noted that the modification of the crystallites existing in the HAD fibers could be the α-form only. Nagai et al. [15] found that the as-spun PEN fibers obtained above 4,000 m/min had (020) and (200) reflections due to β-form, and that the β-form transferred to α-form during hot-drawing.

In Fig. 8, the melting points (T_m) of the HAD fibers obtained under various conditions are plotted as a function of $\dot{\varepsilon}$. T_ms were obtained from d.s.c. curves for the original fiber and the HAD fibers obtained at four different $\dot{\varepsilon}$s. The original fiber shows a broad exothermic transition at 217°C caused by cold crystallization; and a melting endotherm peaking at 268°C. The HAD fibers have only a single sharp endotherm peak due to melting. T_m increases at first with increasing $\dot{\varepsilon}$, and leveling off occurs at high $\dot{\varepsilon}$. The HAD fibers obtained at $\dot{\varepsilon} = 25.2\ s^{-1}$ have T_m = 274°C, which is slightly lower than that (T_m = 276°C) of the zone-drawn/zone-annealed PEN fiber [16]. Buchner et al. [11] reported that the fiber of the α-form had T_m = 278°C when it crystallized at 207°C for 2 h and was annealed at 269°C for 40 min. In high speed spinning of PEN [14], the melting point increased with the spinning speed, and the as-spun fiber obtained at 5,000 m/min had the melting endotherm peaking at 292°C. The fibers spun with a high speed had the melting peak attributed to the β-form. Although both α- and β-crystal forms have almost the same T_m, the melting peaks of the HAD fibers are due to the melting of the α-form of crystallites because no β(020) reflection is observed in Fig. 7(a) and (b). The changes in the profiles of the melting peaks with $\dot{\varepsilon}$ are attributed to an increase in crystal size and/or crystal perfection [28,29], thus being supported by the X-ray observation.

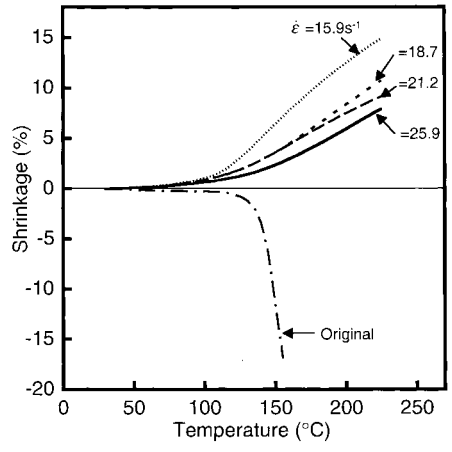

Fig. 9. Temperature dependence of thermal shrinkage for the original and HAD fibers obtained at four different strain rates.

Fig. 9 shows the temperature dependence of the thermal shrinkage for the original fiber and the HAD fibers obtained at four different $\dot{\varepsilon}$s. The thermal shrinkage during heating is associated with the chain coiling in the oriented amorphous regions [30] and is also dependent on the orientation of amorphous regions and the degree of crystallinity. The original fiber stretches so rapidly above 140°C that the stretch exceeds the present instrumental limitation. The rapid stretch of the original fiber shows that no network preventing the fluid-like deformation exists, and that no strain-induced crystallization occurs during the measurement.

On the other hand, the HAD fibers start to shrink above 50°C as the temperature increases. The slight increase is attributable to a β-relaxation. The β-relaxation is associated with the motion of the naphthalene rings; the motion appears to involve rotations around the nearest oxygen–naphthyl links which are aligned along the main chain axis of the polymer [31]. Each of the HAD fibers shrinks gradually with temperature, and the HAD fiber obtained at $\dot{\varepsilon} = 25.2\ s^{-1}$ shows the lowest attainable shrinkage of the HAD fibers. This difference in the behavior of the shrinkage among the HAD fibers is due to the difference of the crosslink density of the physical network built up by the crystallites. Therefore the physical network in the HAD fiber obtained at lower $\dot{\varepsilon}$ was less sufficient for constraint of the thermal shrinkage because of its low X_w. On the other hand, in the fiber obtained at $\dot{\varepsilon} = 25.2\ s^{-1}$ the crosslink density of the physical network, which restricts most highly the chain coiling, found to be the highest among the HAD fibers drawn at various $\dot{\varepsilon}$s.

3.2. Mechanical properties of HAD fibers under various conditions

Fig. 10(a) and (b) show the tensile modulus and tensile strength plotted against $\dot{\varepsilon}$ for the HAD fibers obtained under various conditions. The tensile modulus and tensile strength increase with $\dot{\varepsilon}$, and the HAD fiber obtained at $\dot{\varepsilon} = 25.2\ s^{-1}$ has a tensile modulus of 29 GPa and a tensile strength of 0.97 GPa, which are almost the same values as those of the zone-annealed PEN fiber [16]. Nagai et al. [14] reported that when the as-spun PEN fiber obtained at 5,000 m/min was drawn three times at 155, 190, and 220°C, the drawn fiber had a tensile modulus of 30 GPa and tensile strength of

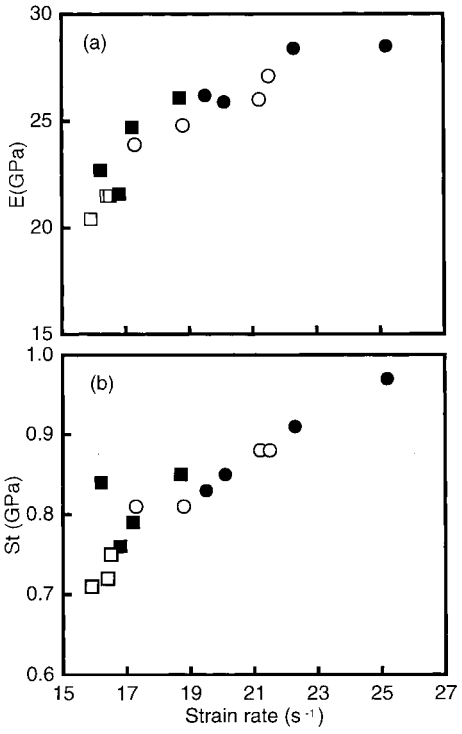

Fig. 10. (a) Tensile modulus (E) and (b) tensile strength (St) plotted against strain rate for the HAD fibers obtained under various conditions: (□) T_d = 150°C; (■) T_d = 200°C; (○) T_d = 230°C; (●) T_d = 250°C.

0.96 GPa. Nakamae et al. [32,33] reported that the elastic modulus (E_l) of the crystalline regions of the PEN in the direction parallel to the chain axis was 145 GPa at room temperature, and that the E_l value was constant in the 22 to 228°C range.

Figs. 11 and 12 show the temperature dependence of the storage modulus (E') and loss tangent (tan δ) for the original fiber and HAD fibers obtained at four different $\dot{\varepsilon}$s. The E' value over a wide temperature range increases with $\dot{\varepsilon}$, and E' of the HAD fiber at $\dot{\varepsilon} = 25.2\ s^{-1}$ reaches 30 GPa at 25°C.

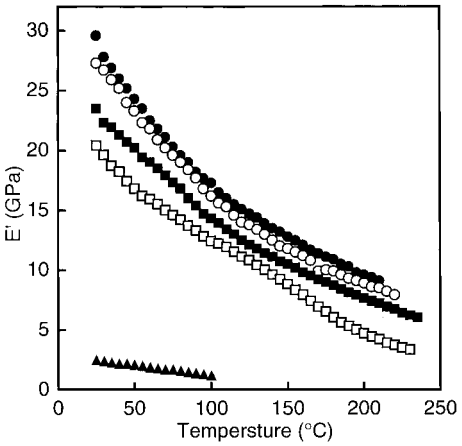

Fig. 11. Temperature dependence of storage modulus (E') for the original fiber and the HAD fibers obtained under four different strain rates ($\dot{\varepsilon}$): (▲) original; (□) $\dot{\varepsilon} = 15.9\ s^{-1}$; (■) $\dot{\varepsilon} = 18.7\ s^{-1}$; (○) $\dot{\varepsilon} = 21.2\ s^{-1}$; (●) $\dot{\varepsilon} = 25.2\ s^{-1}$.

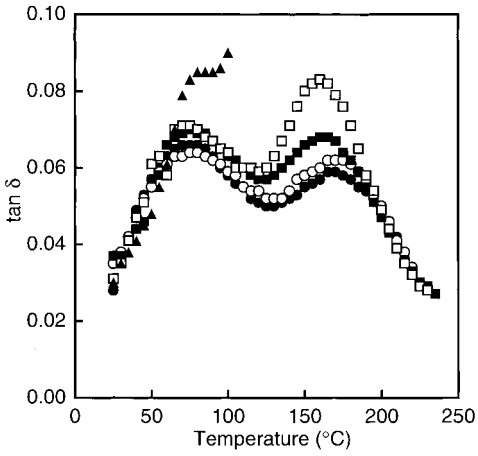

Fig. 12. Temperature dependence of tan δ for the original fiber and the HAD fibers obtained under four different strain rates ($\dot{\varepsilon}$): (▲) original; (□) $\dot{\varepsilon} = 15.9\ s^{-1}$; (■) $\dot{\varepsilon} = 18.7\ s^{-1}$; (○) $\dot{\varepsilon} = 21.2\ s^{-1}$; (●) $\dot{\varepsilon} = 25.2\ s^{-1}$.

The tan δ vs. temperature curves for the HAD fibers show peaks of β-relaxation at about 70°C and α-relaxation at about 170°C. The α-relaxation is considered to correspond to the glass transition [29]. The α-relaxation peak decreases in their peak heights, shifts to a higher temperature, and becomes much broader as $\dot{\varepsilon}$ increases. The changes in position and in profile of the α-peak with $\dot{\varepsilon}$ indicates that the molecular mobility in the amorphous regions is restricted by the physical network with a high degree of crosslink density.

4. Conclusions

HA drawing was applied to PEN fiber, and the drawing was carried out at various temperatures and applied tensions. The fiber was rapidly drawn by the HA drawing. The strain rate increased as the drawing temperature and applied tension increased. The maximum strain rate was $25.2\ s^{-1}$, which was obtained at a drawing temperature of 250°C and applied tension of 17.4 MPa. The draw ratio, birefringence, and orientation factor of the crystallites increased as the strain rate increased, and these changes of the HAD fibers depended markedly on the strain rate. The HAD fiber drawn at the maximum strain rate had a birefringence of 0.436 and degree of crystallinity of 45%, and the degree of crystallinity was much higher than that of the zone-annealed PEN fiber. Mechanical properties also increased with the strain rate, and the fiber drawn at $25.2\ s^{-1}$ had a tensile modulus of 29 GPa and a tensile strength of 0.97 GPa. In addition to the condition that the time required for drawing was extremely short, the hot-air drawing method was found to be effective in the improvement of the mechanical properties of the PEN fibers. Generally speaking, when amorphous polymer was drawn at high temperatures close to melting point, the intermolecular linkages are broken down, and as a result the polymer molecules may slip past one another and flow individually,

exhibiting a large deformation without inducing any molecular orientation and crystallization [26]. However, the instantaneous heating by blowing hot-air regulated previously at high temperature permitted development of molecular orientation and crystallization without flow drawing due to chain slippage.

Acknowledgements

We are grateful to Teijin Ltd. for supplying PEN fibers to us.

References

[1] Acierno D, La Mantia FP, Polizotti G, Alfonsoand GC, Ciferri A. J Polym Sci, Polym Lett Ed 1977;15:323.
[2] Zachariades AE, Poter RS. J Appl Polym Sci 1979;24:1371.
[3] Ülçer Y, Çakmak M. Polymer 1994;35:5651.
[4] Lu X, Windle AH. Polymer 1995;36:451.
[5] Murakami S, Nishikawa Y, Tsuji M, Kawaguchi A, Kohjiya S, Cakmak M. Polymer 1995;36:291.
[6] Cakmak M, Lee SM. Polymer 1995;36:4039.
[7] Abis L, Merlo E, Pó R. J Polym Sci Polym Phys Ed 1995;33:691.
[8] Rueda DR, Varkalis A, Viksne A, Calleja FJ, Zachmann HG. J Polym Sci Polym Phys Ed 1995;33:1653.
[9] Zhang H, Rankin A, Ward IM. Polymer 1996;37:1079.
[10] Jakeways R, Klein JL, Ward IM. Polymer 1996;37:3761.
[11] Buchner S, Wiswe D, Zachmann HG. Polymer 1989;30:480.
[12] Ghanem AM, Porter GS. J Polym Sci Polym Phys Ed 1989;27:2587.
[13] Ito M, Honda K, Kanamoto T. J Appl Polym Sci 1992;46:1013.
[14] Nagai A, Murase Y, Kuroda T, Matsui M, Mitsuishi Y, Miyamoto T. Sen-i gakkaishi 1995;51:470.
[15] Nagai A, Murase Y, Kuroda T, Matsui M, Mitsuishi Y, Miyamoto T. Sen-i gakkaishi 1995;51:478.
[16] Suzuki A, Kuwabara T, Kunugi T. Polymer 1998;39:4235.
[17] Kunugi T, Suzuki A, Hashimoto M. J Appl Polym Sci 1951;1981:26.
[18] Suzuki A, Murata H, Kunugi T. Polymer 1998;39:1351.
[19] Suzuki A, Sato Y, Kunugi T. J Polym Sci, Polym Phys Ed 1998;36:473.
[20] Kunugi T, Suzuki A. J Appl Polym Sci 1996;62:213.
[21] Mencik Z. Chem Prumysl 1967;17:78.
[22] Ouchi I, Aoki H, Shimotsuma S, Asai T, Hosoi M. In: Proceedings of the 17th Congress on Materials Research, Japan, 1974, p. 217.
[23] Wilchinsky ZW. J Appl Phys 1963;30:792.
[24] Aikawa Y. Koubunshi Ronbunsyu 1994;51:237.
[25] O'Neill MA, Duckett RA, Ward IM. Polymer 1988;29:54.
[26] Ajji A, Guèvremont J, Cole KC, Dumoulin MM. Polymer 1996;37:3707.
[27] Ülçer Y, Cakmak M. Polymer 1997;38:2907.
[28] Mandelkern L, Price JM, Gopalan M, Fatou JMG. J Polym Sci 1966;4:385.
[29] Taraiya AK, Unwin AP, Ward IM. J Polym Sci Polym Phys Ed 1988;26:817.
[30] Wilson MPW. Polymer 1974;15:277.
[31] Blundell DJ, Buckingham KA. Polymer 1985;26:1623.
[32] Nakamae K, Nishino T, Tada K, Knamoto T, Ito M. Polymer 1993;34:3322.
[33] Nakamae K, Nishino T, Gotoh Y. Polymer 1995;36:1401.